minerals

MDPI

Article

About the Origin of Carbonado

Valentin Afanasiev [1,*], Vladimir Kovalevsky [2], Alexander Yelisseyev [1], Rudolf Mashkovtsev [1], Sergey Gromilov [3,4], Sargylana Ugapeva [5], Ekaterina Barabash [1], Oksana Ivanova [1] and Anton Pavlushin [5]

1 Sobolev Institute of Geology and Mineralogy, Siberian Branch of the Russian Academy of Science, Novosibirsk 630090, Russia; eliseev.ap@mail.ru (A.Y.); rim@igm.nsc.ru (R.M.); hyperborean@bk.ru (E.B.); ksu_88@bk.ru (O.I.)
2 Geological Institute of Kola Science Centre, Russian Academy of Sciences, Apatity 184209, Russia; kovalevs@krc.karelia.ru
3 Nikolaev Institute of Inorganic Chemistry, Siberian Branch, Russian Academy of Sciences, Novosibirsk 630090, Russia; grom@niic.nsc.ru
4 Department of Physics, Novosibirsk State University, Novosibirsk 630090, Russia
5 Diamond and Precious Metal Geology Institute, Siberian Branch, Russian Academy of Science, Yakutsk 677000, Russia; ugapyevass@diamond.ysn.ru (S.U.); pavlushin@diamond.ysn.ru (A.P.)
* Correspondence: avp-diamond@mail.ru; Tel.: +7-(913)-910-46-95

Abstract: Carbonado is a specific variety of diamonds, typical representatives of which are distributed in the diamond placers of Central Africa, Brazil, and Venezuela. Carbonado consists of the microcrystalline aggregates of diamonds, with inclusions of mineral matter. These aggregates appear as fragments that are rounded to varying degrees. Carbonado has been known for a long time, but its primary sources have not been found and its genesis remains unclear. We have substantiated the hypothesis that the most probable precursor of carbonado is shungite. Shungite is a specific form of non-crystalline, non-graphitic, fullerene-like carbon. Shungite rocks, currently known in Karelia (Russia), are natural microdispersed composite materials containing shungite—carbonaceous matter and mineral components of different compositions. The content of carbonaceous matter in shungite rocks is from less than 10% to 98%. The carbon isotopic composition of shungite is light $\delta^{13}C$ from −25‰ to −40‰. The age of shungite rock is more than 2 billion years old, but earlier shungite was probably much more widespread. Known shungite rocks are more than 2 billion years old, but earlier shungite was probably much more widespread. Shungite rocks could recrystallize into diamond rock upon subduction to high pressure and temperature. The diamond rocks could then be exhumed to the Earth's surface, where they could undergo disruption and reworking with formation of those very fragments that are known as "carbonado".

Keywords: diamond; carbonado; shungite; subduction; exhumation

Citation: Afanasiev, V.; Kovalevsky, V.; Yelisseyev, A.; Mashkovtsev, R.; Gromilov, S.; Ugapeva, S.; Barabash, E.; Ivanova, O.; Pavlushin, A. About the Origin of Carbonado. *Minerals* **2024**, *14*, 927. https://doi.org/10.3390/min14090927

Received: 18 July 2024
Revised: 30 August 2024
Accepted: 30 August 2024
Published: 11 September 2024

1. Introduction

Carbonado is a black micropolycrystalline variety of diamond containing numerous inclusions of various minerals. The term was coined by Brazilian miners in 1840 to describe the black, brown, gray, irregularly shaped diamond outcrops that differ sharply from ordinary diamonds [1]. Carbonado was later found in Venezuela and in the Central African Republic. In recent decades, there have been reports of polycrystalline diamonds attributed to carbonado in other locations and different geological settings [2–8]. Debye rings on X-ray radiographs (lauegrams), indicating micropolycrystallinity, served as the main diagnostic sign of carbonado. As a result, a variety of microcrystalline diamond varieties differing in origin, properties, and age were attributed to carbonados, which resulted in complete uncertainty in the genesis of carbonados. Thus, yakutites found in placers of the northeastern Siberian Platform [9] were called "carbonado with lonsdaleite" [2,10], which led to the assumption that carbonados are related to impact events. However, it was already stated in the paper [5] that yakutites are not carbonado, and the genesis of carbonado is

not clear. B. Smith and J. Dawson also suggest the connection of carbonado with impact events [4]. H. Kagi and F. Kaminsky assume the role of a radiogenic factor [11,12]. A similar point of view is expressed by [13]. References [3,7,8,14] indicate that carbonados are present in Phanerozoic kimberlites and are associated with the upper mantle, but again, the diagnosis is based only on the microgranularity of these diamonds. F. Kaminsky and E. Francesson formulated the viewpoint of a crustal source of material for carbonados [15]. A similar point of view is formulated in [16]. Carbonados were also noted in the avachites of Kamchatka [6]. Regarding diamonds in Kamchatka, it should be noted that no diamond finds in association with volcanoes have been reproduced, and if the genetic hypotheses formulated in connection with these "finds" were real, Kamchatka would be studded with diamonds [17]. Carbonado age estimates from published works vary from Phanerozoic to deep Precambrian, but the Pb-Pb ages of quartz and rutile inclusions in a Brazilian carbonado have an isochron age of 3315 ± 720 Ma, and an age of 3811 ± 1800 Ma has been determined for the carbonado matrix; the ages of Brazilian carbonados are indicated to be consistent with those of African carbonados [18].

The cited literature strongly suggests that many reported carbonado occurrences do not comprise real carbonado. As a result, there remains some confusion regarding the genetic hypotheses and geological setting for carbonado formation.

In this regard, the very term "carbonado" must be clearly defined before any characterization study is carried out. In our opinion, only the typical carbonados from Brazil, known since 1840, can be called carbonados. Other "carbonado" occurrences need to be verified in a comprehensive comparison with these ones. Carbonados are endemic. Within Gondwana, the area of the distribution of carbonados in Brazil and Africa was unified, and only after the breakup of Gondwana and the opening of the Atlantic in the Mesozoic was this area divided. The polycrystalline diamonds that are completely similar to typical carbonado diamonds are not found anywhere in the world (at least, there is no reliable information about such finds). If one is to claim to find carbonados outside the present area of their distribution, it is necessary to show a full analogy with typical carbonados using a wide range of studies.

S. Haggerty also studied carbonados from Brazil and Africa [19,20]. In these papers, he describes carbonados in detail and also provides the most comprehensive review of hypotheses regarding the genesis of carbonados. S. Haggerty distinguishes five groups of hypotheses:

1. Meteoritic impact [4];
2. Growth and sintering in the crust or mantle [21–25];
3. Subduction [16,26,27];
4. Radioactive ion implantation of carbon substrates [11–13,28–30];
5. Extraterrestrial [19,31].

He notes that although carbonado is well studied, its genesis remains unknown. Regarding his hypothesis, S. Haggerty points out that it will be confirmed only by the discovery of carbonados in the asteroid belt via remote sensing or by finding a diamond meteorite corresponding to a carbonado.

We also believe that the issue of carbonado genesis is still unsolved and propose our hypothesis of carbonado formation. In this article, the typical carbonados from Brazilian placers are described, and on the basis of these studies, the most probable precursor of these diamonds is determined, and their genesis is discussed. Only data from the literature that relate to genuine carbonados are used.

As it was stated above, the carbonados are found only in the placers of Brazil, Venezuela, and Equatorial Africa. The size ranges from a millimeter to several centimeters; the largest carbonado found in Brazil weighed 3167 carats [1]. As a rule, it is porous. The pores, both on the surface and inside, are occupied by a variety of minerals, the list of which is very extensive and varies among various authors. Thus, according to the data of [18], rutile, florensite, quartz, zircon, and clay minerals are described, which indicate a crustal source. F. Trueb et al. [18,32] diagnosed allanite, anhydrite, galena, helenite, hematite,

goethite, ilmenite, kaolinite, cassiterite, quartz, covellite, monazite, orthoclase, parisite, perovskite, pseudomalachite, rutile, serpentine, chloritoid, chromospinelide, zircon, and florensite. A.I. Gorshkov and his colleagues describe goyacite; rutile; nugget metals—iron, chromium, Fe-Cr solid solutions, titanium, copper, gold, silver, and a solid solution of gold and silver; and argentite sulfide as inclusions [14,33]. F. Kaminsky identified garnet, apatite (including fluorapatite), phlogopite (or high-silica), SiO_2, and Ca-Mg-Sr- and Ca-Ba-carbonates; halides (KCl and BiOCl); nugget Ni and metal alloys (Fe-Ni, Cr-Fe-Mn and Pb-As-Mo); oxides (FeO, Fe-Sn-O, TiO_2, SnO_2, and PbO_2) and Fe-sulfides; and fluid inclusions [34]. The following nitrides were also found: Ti_3CuN, $TiCuN_2$, and Cu_3N [35]. The inclusions of highly baric minerals typical of mantle diamonds from kimberlites were not identified. The carbon isotopic composition of carbonado is light $\delta^{13}C$ 27.8‰–28.1‰, as reported in [36], and 29.2 and 30.6‰, as reported in [37]. The density varies from 3.13 to 3.46 g/cm^3 depending on the degree of porosity [37]. The age of the carbonado is Archean, and available isotopic dating indicates ages greater than 3 billion years [38].

In this study, the results of our research on true carbonados from Brazil are shown, and a new hypothesis regarding the genesis of carbonados is proposed, which consolidates known information about these unusual diamonds in a consistent manner.

2. Materials and Methods

Research was carried out on our collection of carbonados from Brazilian placers, totaling five samples. The specimens were donated to us by a Brazilian colleague in 2013; their exact location within Brazil is not known.

The morphology of the samples was investigated via optical microscopy. A MIRA 3 LMU scanning electron microscope (Tescan Ltd., Brno, Czech Republic) was used at the Institute of Geology and Mineralogy of the Siberian Branch of the Russian Academy of Sciences to study the microrelief. The surface of the samples was cleaned in an autoclave [39], which allowed us to "look" into the pores cleaned from minerals on the surface of the samples using a scanning electron microscope.

To study the orientation of carbonado subgrains, diffraction analyses of electron backscattering (EBSD) were used at MQ University, Australia, in 2014. To carry out investigations with this method, a plate was laser cut from one of the samples (Figure 1 bottom right) and polished. Operating at 20 kV, a working distance of 10 mm and a sample tilt of 70° in the high vacuum mode were used on carbon-coated samples. Patterns were acquired on rectangular grids by moving the electron beam at a regular step size of 1 micron.

Figure 1. Morphology of the studied Brazilian carbonado specimens (collection of the Institute of Geology and Mineralogy of the Siberian Branch of the Russian Academy of Sciences).

The X-ray diffractometer BrukerDUO (MoKα-radiation, graphite monochromator, and CCD-detector) at the Institute of Inorganic Chemistry, Siberian Branch of the Russian Academy of Sciences, was used to examine the ~0.5 mm sample.

The photoluminescence (PL) spectra were measured at the Institute of Geology and Mineralogy of the Siberian Branch of the Russian Academy of Sciences using an SDL1 luminescence spectrometer with excitation from a pulsed Nd:YLF DPSS laser DTL-399QT at 527 and 351 nm. To record the PL emission, we used a cooled FEU83 photomultiplier, which is sensitive within the 350 to 1200 nm range. The PL spectra were measured at liquid nitrogen temperatures using a metal vacuum cryostat with quartz windows.

EPR spectra were measured at the Institute of Geology and Mineralogy of the Siberian Branch of the Russian Academy of Sciences at room temperature (RT) and on a Radiopan SE/X 2543 spectrometer with a built-in NMR magnetometer. The output EPR signal was digitized with a custom-made 16-bit ADC that interfaced with a PC. When the spectra of defect centers with narrow lines were collected, microwave power was reduced to avoid any signal saturation. The amplitudes of 100 kHz with respect to modulation and the gain coefficients (K) used for EPR signal detection were selected as 0.025 G, K = 5×10^2 and 0.32 G, K = 2×10^3 for the central region of EPR spectra (g~2.002) and triplet-type defects, respectively. A computer simulation of the EPR spectra was performed using the EPR-NMR program, which allows modeling transitions $\Delta M_S = 1, 2$ with correct intensity ratios between them. The total spin concentration was compared with the spin concentration in the reference sample (DPPH powder with 5×10^{15} spins). A comparison was performed using the double integration of the EPR spectra.

3. Results

3.1. Carbonado Morphology

The studied samples, 3–9 mm in size, have the form of irregularly shaped fragments. The fragments are variously rounded, and some are egg-shaped (Figure 1).

The color of the sample is black, brown, or dark gray. The size of diamond crystallites comprising the carbonado, according to EBSD data, is different within the sample—from the first tens of microns to submicroscopic. All samples show pores filled with mineral matter on the surface. One of the samples was cleaned in an autoclave to remove the substance from the pores [39]. Octahedral diamond crystals the size of a few microns are visible on the pore walls after the removal of minerals (Figure 2).

3.2. EBSD

Via the EBSD method, it was found that crystallites on the surface of the polished plate have an area of 10–60 μm^2 and are irregularly shaped, and large and small grains are grouped in clusters throughout the sample (Figure 3).

Some grains show signs of plastic deformation in the form of fragmentation into subgrains, with maximum angles of disorientation up to 7°. No predominant crystallographic orientation of grains is observed over the whole investigated area of the carbonado sample (see also Figure 2).

3.3. X-ray Diffraction Study

The inserts in Figure 4 show the following: a—the sum of 77 debaegrams obtained by summing a series of frames obtained at different positions of the sample relative to the primary beam; b—the diffraction pattern of a stationary sample (lauegram). The measured unit cell parameter 3.566 A coincides with the reference value of 3.567 A.

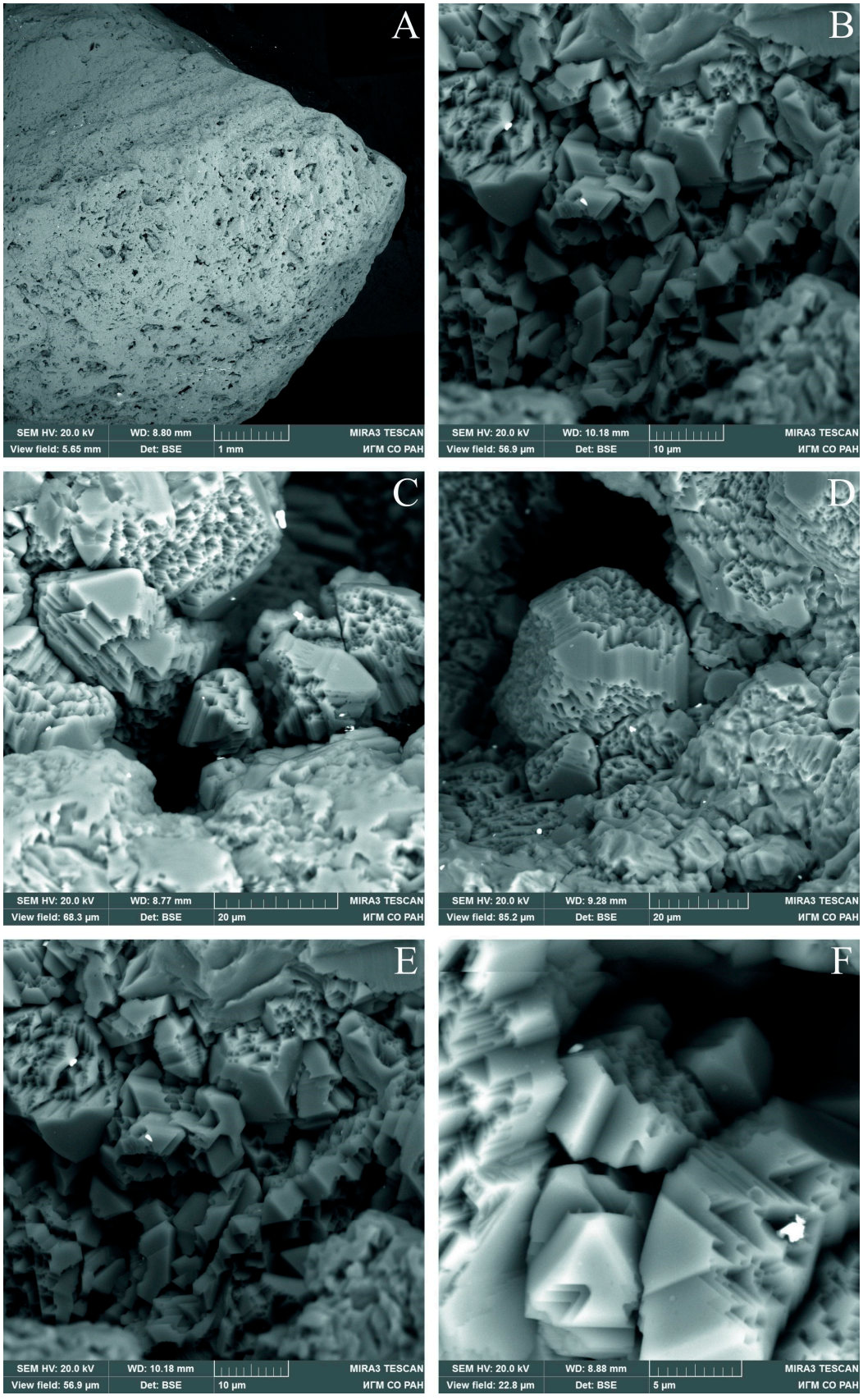

Figure 2. SEM images of diamond crystallites in pores cleaned from mineral matter. (**A**) fragment of a studied carbonado with pores; (**B**–**F**) diamond crystallites in pores at different magnifications.

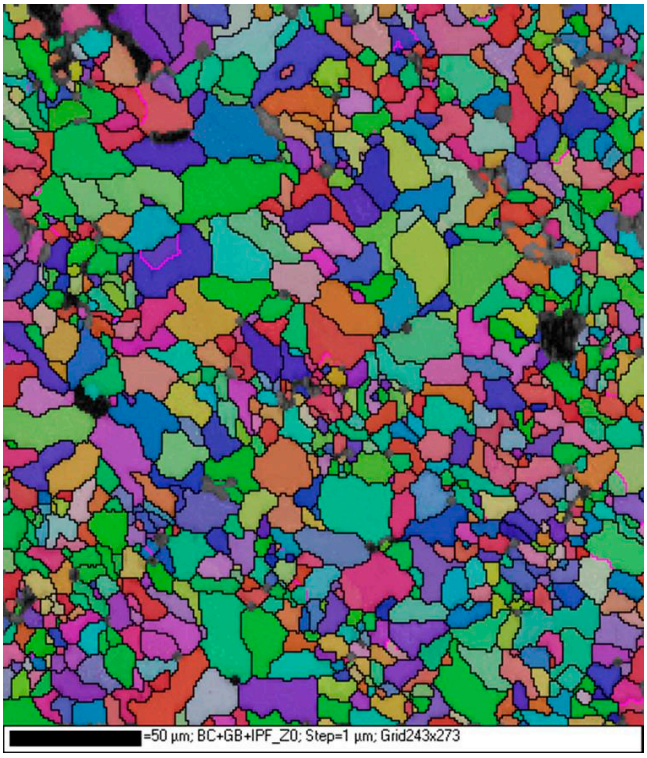

Figure 3. EBSD map of the polished carbonado. Different colors indicate different crystallographic orientations.

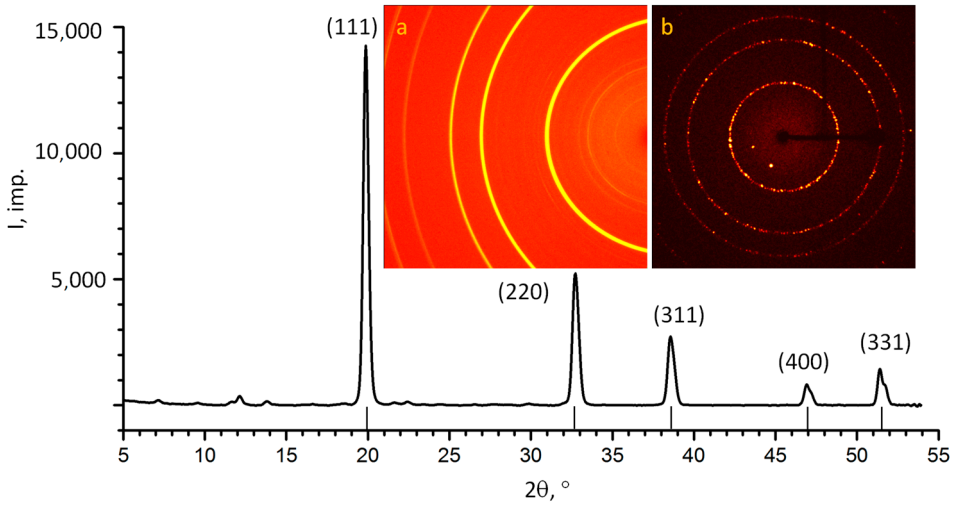

Figure 4. X-ray diffraction patterns of carbonado (MoKα). The strokes near the horizontal axis show the theoretical positions of the diamond reflexes (unit cell parameter a = 3.567 Å). The inserts show the original diffraction patterns: a—the sum of 77 debaegrams; b—the lauegram.

3.4. Photoluminescence (PL)

Figure 5 shows the unit-normalized low-temperature PL spectra measured at excitation wavelengths of 351 nm (1 and 1a). Two vibronic systems (VSs) with zero-phonon lines (ZPLs) of 503.2 and 575.0 nm dominate in the PL spectrum under UV excitation (curve 1) (Table 1).

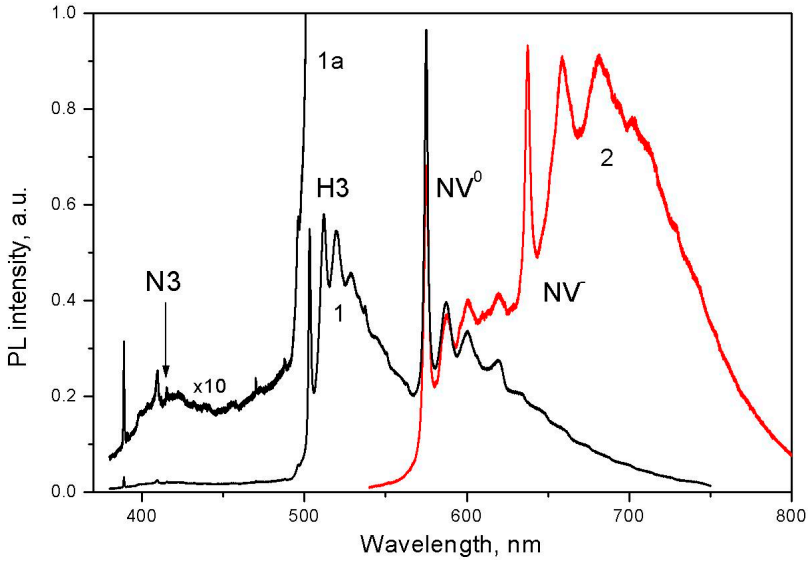

Figure 5. The PL spectra for carbonado obtained at 77 K and at 350 nm (1, 1a) and 527 nm (2) excitations. The details of the spectrum (1) within the range of 370–500 nm is shown with 10-fold magnification (1a).

Table 1. Parameters of zero-phonon lines in the PL spectra of carbonado.

NN	ZPL Position		FWHM, meV	Center Title	Center Structure
	Wavelength, nm	Photon Energy, eV			
1	388.8	3.188	7.0		
2	415.2	2.985	7.2	N3	N_3V
3	503.2	2.463	7.2	H3	NVN
4	575.0	2.155	9.0	center 575	NV^0
5	637.5	1.945	13.0	center 638	NV^-

Here N is a nitrogen atom and V is a vacancy. FWHM is the full width at half-maximum.

In the short-wavelength region of the spectrum (in the range of 370–500 nm), a slightly significantly weaker vibronic system is observed in the PL spectrum with a ZPL of 388.8 nm with phonon replicas at 398.5 and 409.5 nm, as well as ZPLs at 415.2, 470.1 and 487.8 nm. The PL spectrum obtained at 527 nm excitation is dominated by ZPLs at 575.0 nm and 637.5 nm. The parameters of the main ZPLs are given in Table 1.

All mentioned systems are well known for diamonds and belong to various nitrogen–vacancy complexes. The simplest of them are nitrogen–vacancy N-V complexes: neutral (center 575) and negatively charged complex (center 638). There are also complexes containing two nitrogen atoms (H3 center with ZPL 503.2 nm) and three nitrogen atoms around a carbon vacancy (N3 center with ZPL 415.2 nm) [40].

With respect to the system with a ZPL of 388.8 nm, it is associated with a radiation defect that is observed in all types of nitrogen-containing diamonds after irradiation with ions or electrons. Various authors have suggested that it is a complex involving an interstitial or substitutional nitrogen atom [40]. Narrow lines of 470.0 nm and 487.9 nm are associated with pure radiation defects TR12 and TH5. The first of them presumably includes two vacancies and two interstitial carbon atoms [41], while the other is surmised to be an intrinsic defect containing a divacancy [40,42]. In perfect single crystals of diamonds, whether natural or synthetic, ZPLs are significantly narrower (FWHM is less than 1 meV). In carbonado, the ZPLs are significantly broadened from 7 to 13 meV, which indicates strong deformations in the structure. The relatively low degree of nitrogen aggregation and the presence of only one or two nitrogen atoms in the structure of nitrogen defects indicate

the relatively low annealing temperatures of the diamonds (at the level of 1500–1600 °C). It is assumed that high-temperature annealing is possible at higher temperatures when a higher degree of nitrogen aggregation is achieved: Nitrogen centers containing a larger number (three or four) nitrogen atoms are formed, namely centers such as N_3V or B-centers, respectively. The presence of TH5 centers indicates annealing at T > 400 °C after irradiation [41].

3.5. EPR Spectra

Several paramagnetic centers were detected in the EPR spectra recorded in the g~2 region, as shown in Figure 6a. The well-known center P1 (a single substituent nitrogen atom in the diamond structure) and a strong slightly asymmetric line at g = 2.0024 are visible. The total concentration is Ns = 2.4×10^{18} spins/g, and the P1 concentration is equal to 1.5×10^{17}/g, i.e., it is quite low.

Table 2. EPR parameters for defects with S = 1 and S = 3/2 observed in carbonado. Experimental g_{hf} values were determined for a frequency of 9264 MHz.

Center	*S*	g_1	g_2	g_3	g_{hf}	D_1	D_2	D_3	References
			$\Delta M_S = 1$		$\Delta M_S = 2$		MHz		
R1	1	2.0019	2.0020	2.0027	4.704	−2805.6	1408.6	1396.8	[43]
W15/NV	1		2.0028		4.287	1916	−958	−958	[41]
NM1	3/2	2.0002	2.0220	2.0220		1065.7	−532.8	−532.8	
NM2	1		2.0028		4.460	2350	−1170	−1180	

Figure 6b shows a trial simulation of the central line. However, a comparison of the experimental line and the total line modeled using two additional lines with the unchanged P1 line in Figure 6a shows significant differences. Obviously, it was impossible to obtain an asymmetric line from three symmetrical lines. In addition, two poorly expressed shoulders with a splitting of approximately 6 G are visible in the experimental spectrum, which we find difficult to model using known defects. However, in addition to this pair of shoulders, it is obvious that the contribution of other undetected defects leads to the asymmetry of the experimental line.

Figure 6c shows the EPR spectrum recorded in the extended range with a gain coefficient of 2×10^3 and microwave modulation of 0.32 G. Compared to the P1 center, very weak lines from three defects were found, which are described by the spin Hamiltonian:

$$\mathcal{H} = \beta_e \mathrm{B} \cdot \mathrm{g} \cdot \mathrm{S} + \mathrm{S} \cdot \mathrm{D} \cdot \mathrm{S} \quad (1)$$

with an electron spin of S = 1 or 3/2.

We identified two defects R1 and W15 by modeling the resonance lines for these defects with an electron spin of S*S* = 1 using the spin Hamiltonian parameters published in [43–45] (Table 2). However, for two relatively narrow and more intense lines next to the W15 lines (see Figure 6), it was not possible to find an explanation using the spin Hamiltonian parameters published to date. We assumed that four lines belonged to an unknown defect (designated as NM1 with spin S = 3/2), taking into account the third line observed on the flank of the high field of the center P1, and the fourth line is possibly hidden by the flank of the low field of the center P1. The EPR spectrum of the NM1 defect is modeled using the spin Hamiltonian given in Table 2. Our assumption is confirmed by the observation of "forbidden" $\Delta Ms = 2$ transitions in the half-field region shown in Figure 6d for the centers R1 and W15 with S = 1, but not for the center NM1 with S = 3/2. Assuming the electron spin *S* = 1 for the NM1 center, the transition $\Delta Ms = 2$ would be observed near the W15 line.

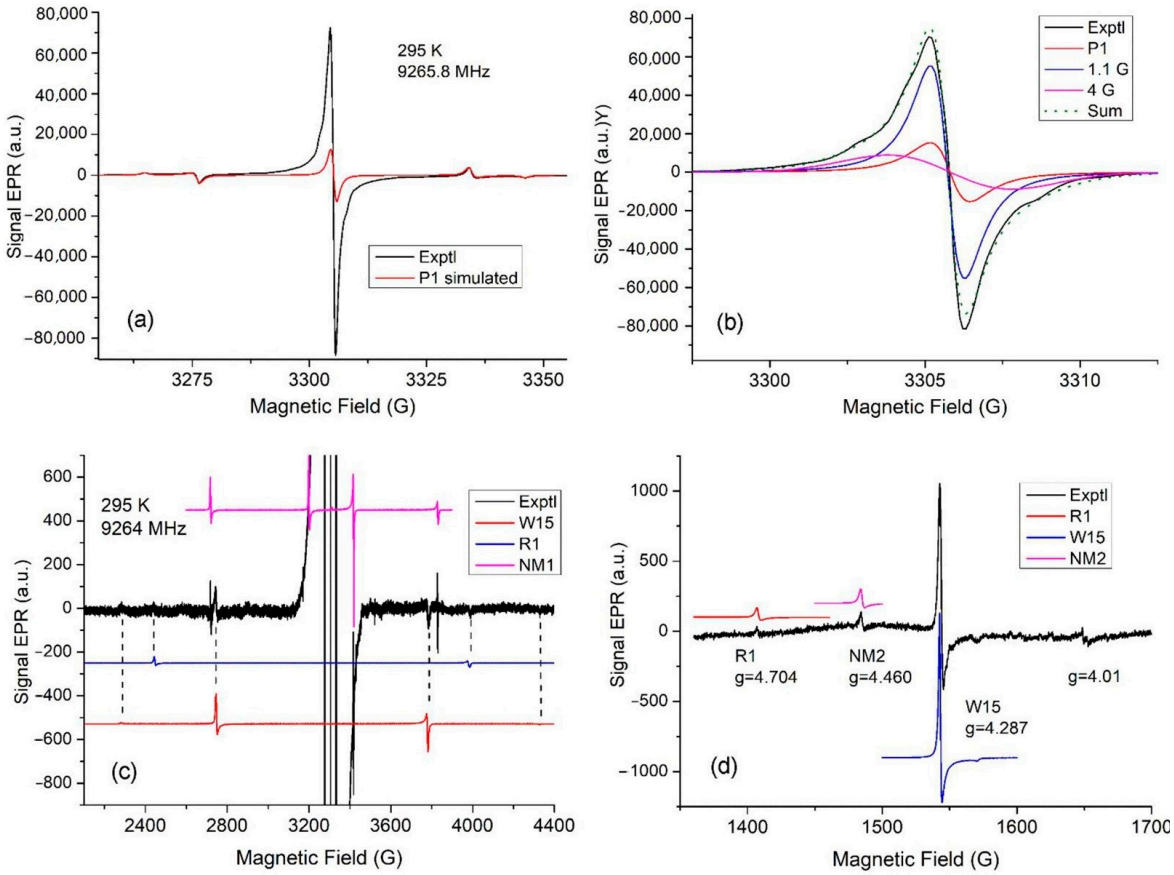

Figure 6. A typical EPR spectrum of studied carbonado. (**a**) Experimental EPR spectrum of carbonado in the central region (black trace). A computer simulation of the EPR spectrum for the P1 center is also shown (in red). (**b**) Simulation of the strong main line using the P1 center (red) and two components: Lorentzian with g = 2.0027, width at ΔH_{pp} = 1.1, and Gaussian at g = 2.0026, ΔH_{pp} = 4.0 G (blue and magenta curves). Their weighted sum (dotted curve) is also shown. (**c**) Experimental EPR spectrum of carbonado in the extended range (black trace). Computer simulations of EPR spectra for defects R1, W15, and NM1 (in red, blue, and magenta colors) are also shown. (**d**) Half-field region of the experimental EPR spectrum (black trace) of spin-triplet-type centers (the gain coefficient and modulation amplitude are the same as in (**c**)). Computer-simulated spectra (red, blue, and magenta curves) were obtained for defects R1, W15, and NM2 using the spin Hamiltonian parameters given in Table 2.

The resonance lines for the "forbidden" transitions ΔMs = 2 turned out to be more intense than for ΔMs = 1. This made it possible to find a resonance line with g = 4.460 in the half-field region for the new NM2 center, which has not been published to date. To model the new line, we used the spin Hamiltonian parameters given in Table 2. These parameters were chosen based on the parameters of the centers R1 and W15. The modeling of EPR spectra for the NM2 center shows that at $D_2 = D_3$, the main pair of allowed lines is only about two times less intense than the "forbidden" transition and should have been observed. Because ΔMs = 1 transitions for the NM2 center were not observed, $D_3 - D_2 \geq 10$ since, under this condition, the allowed transitions have significantly lower intensity relative to the "forbidden" ones.

Additionally, a defect with a narrow weak line at g = 4.01 may correspond to a spin-triplet type center with D_1~300 MHz. We can find a large number of centers with a similar D_1 in [45]. In a wide variety of nanodiamond samples, the spin-triplet-type defects were identified only due to "forbidden" transitions ΔMs = 2 without observed ΔMs = 1 transitions, which turned out to be too weak in intensity [46,47].

4. Discussion

In the discussion of the genesis of carbonados, there are three important characteristics that were not sufficiently considered earlier.

Firstly, carbonado samples, both studied by us and presented in the literature [18,19,22,32,38,48], have the form of fragments, which indicates that they are pieces of a large geological body rather than independent aggregates. The size of this body can be judged from the gigantic area of distribution of carbonados in Africa and Latin America.

Secondly, all carbonado samples have different degrees of mechanical wear, from relatively weak, not hiding their clastic shape, to extremely pelletized (Figure 1). Given the extremely high abrasion resistance of carbonado, far exceeding that of single-crystal diamonds, this degree of wear indicates its antiquity, which is consistent with the age of carbonado [38]. We came to a similar conclusion for the samples of the diamonds of the V variety according to the classification of Yu.L. Orlov [10], also exhibiting high abrasion resistance due to the defectivity of their structure; we hypothesize that these diamonds have the longest exogenous history among the diamonds of the Siberian Platform [49].

Thirdly, the real carbonados are an endemic variety of diamond; they are distributed only in the areas of Brazil, Venezuela, and Central Africa, which were united within Gondwana and separated only in the Mesozoic due to the opening of the Atlantic.

These facts, as well as the whole complex of the studied properties of carbonado, suggest that the most likely protoliths of carbonado were large bodies of geologically old, low-pressure, carbon-rich rocks, which were subducted to great depths into the stability field of diamond and then exhumed to the surface of the Earth. We suggest that these protoliths could correspond to shungite rocks for the reasons explained below.

Shungite is a specific form of carbon, which is a non-crystalline, non-graphitized, fullerene-like carbon, differing from graphite at the level of supramolecular, atomic, and zone (electronic) structure. A characteristic feature of shungites is the presence of smoothly curved carbon (graphene) layers covering nanoscale pores. Shungite rocks are natural composite materials containing shungite, a carbonaceous substance, and various mineral components with compositions ranging from siliceous, aluminosilicate, and carbonate to mixed. In particular, they contain quartz, muscovite, chlorite, albite, calcite, dolomite, and metal sulfides. The carbonaceous content of shungite rocks ranges from less than 10% to 98%. The carbon isotopic composition of shungite is light $\delta^{13}C$ from −25‰ to −40‰. Shungite is more than 2 billion years old [50]. The carbon of shungites with respect to isotopic composition and the forms of accumulation corresponds to organogenic carbon. At present, shungite rocks with reserves of more than 4 billion tons are known to exist in Karelia. Small manifestations of shungites are registered in gold deposits such as “Sovetskoye” on the Yenisei ridge (Russia) and “Eriksson” (Canada), but this rock was probably much more widespread in earlier periods [50].

The morphology and distribution of carbonado, which indicates derivation from a large geological body similar to the shungite field in Karelia; its Archean to Paleoproterozoic age, which is similar to that of known shungite rocks (early Precambrian, probably Paleoproterozoic [50]); and its carbon isotopic composition, which corresponds to organic carbon and is again similar to that of shungite [50] make shungite rocks or their precursors the most likely candidate source of carbonado. In fact, in the Archean and early Proterozoic, there was already life, represented by a massive number of unicellular organisms, due to the fall off, which could form layers of organic matter at the bottom of reservoirs. The authors of [51] indicate the presence of signs of life 3.95 Ga years ago. In the sedimentary process, mineral matter was added to organic matter in variable amounts. Later, these sediments were metamorphosed and turned into shungite or shungite-like rock. It can be assumed that the formed massifs of such rock were subducted into the mantle, where the transformation of shungite carbon into diamond took place and a polycrystalline diamond rock was formed with a variable amount of mineral matter admixture in the form of phenocrysts in the diamond rock. The formation of plate tectonics began about 4 billion years ago and lasted about a billion years [52–54]. For this period, there is evidence of subduction

processes [55]. This formation was then exhumed to the ground surface, similarly to the Kumdy-Kol massifs in Kazakhstan [55,56], or Beni-Bushera in Morocco [57,58], or Ronda in Spain [59]; underwent destruction; and served as a source of carbonado placers. The experimental studies conducted by us have shown that diamond crystallizes from shungite at high pressure (15 GPa) and temperature (1600 °C) within 2 h [60]. However, it is necessary to take into account the time factor, which favors the transformation of shungite into diamond at lower P-T parameters.

The analytical results are in agreement with the formation of carbonado in a subduction environment. All mentioned systems in the PL spectra are similar to ordinary diamonds and belong to various nitrogen–vacancy complexes. The simplest of them is N-V nitrogen–vacancy complexes: neutral (center 575) and negatively charged (center 638). Complexes containing two nitrogen atoms (center H3 with ZPL 503.2 nm) and three nitrogen atoms around the carbon vacancy (center N3 with ZPL 415.2 nm) are also present in the spectra [41]. In perfect diamond single crystals, natural or synthetic, the zero-phonon lines appear to be much narrower (less than 1 meV). In carbonado, ZPLs are significantly broadened from 7 to 13 meV, and this indicates strong deformations in the structure. The EBSD study also demonstrates the same fact.

The PL results show a relatively low degree of nitrogen aggregation and the presence of only one or two nitrogen atoms in the structure of nitrogen defects, which indicates a relatively low temperature of formation and the subsequent existence of carbonado.

As for the system with a ZPL of 388.8 nm, it is attributed to a radiation defect, which is observed in all types of nitrogen-containing diamonds after radioactive irradiation. Various authors have suggested that it is a complex involving an interstitial or substituent nitrogen atom.

The narrow lines at 470 nm and 487.9 nm are attributed to purely radiative defects TR12 and TH5. The former is hypothesized to involve two vacancies and two interstitial carbon atoms [40], while the latter is surmised to be an intrinsic defect containing a divacancy [41]. The TR12 center characteristic of type Ia and IIa diamonds, is well pronounced after heating above 300–600 °C, and is destroyed above 700 °C.

The TH5 center is observed in diamonds of types IIa and Ia after electron irradiation, and it intensifies during annealing at T > 400 °C after irradiation; the destruction of the center occurs at temperatures above 1000 °C [40].

The EPR method reveals the following. An intense central line at g ≈ 2.003 is usually observed in micro-diamonds with a developed surface, and the linewidth is strongly dependent on the sample. In nanodiamonds, the intensity of this line reaches a spin density of about 10^{20} g^{-1} [47]. This line is usually modeled by broad and narrow overlapping lines. It has been suggested that broad and narrow signals are caused by two types of singlet paramagnetic defects (dangling bonds located within the distorted diamond structure), which somehow differ in their origin and location. For example, [61,62] suggested that one paramagnetic center fills the area of the inner surface, and the other center is localized in the outer shell, consisting mainly of non-diamond carbon atoms.

R1 and W15 are typical radiation defects. W15 is a well-studied defect and consists of a vacancy near the nitrogen atom, i.e., NV pair [43]. The NV center is formed in type Ib diamonds after electron or neutron irradiation and annealing at 700 °C, and it is still present after annealing at 1300 °C. R1 is the di-<001>-split interstitial center, which is formed upon electron or neutron irradiation and annealing above 300 °C [44].

From the EPR spectra of powders, it is often difficult to determine the nature of a defect that has not been previously studied in single crystals. But in the case of the NM1 center, there are two signs that suggest the origin of this defect: (i) spin S = 3/2 and (ii) anisotropic g values with $g_{2,3} = g_{\perp}$ are greater than 2. The paramagnetic centers related to nickel all have g values greater than 2. In diamond, only paramagnetic Ni- with configuration $3d^7$ in a structural carbon tetrahedron has S = 3/2 [47,63]. In a regular tetrahedron, an isotropic line at g = 2.0319 is observed, and there is no fine structure expected for all spin states with $S \leq 3/2$ [63]. Therefore, there is a reason for a decrease in the symmetry of

the NM1 defect, which leads to the anisotropy of g values and the appearance of a fine structure. Noble and coauthors suggested that the N^+ ion at the 4nn position is the cause of the observed broad resonance line at g = 2.02, the width of which is partly explained by fine structure and hyperfine splitting from the N^+ ion [47]. In carbonado, Ni-related centers were not previously observed, but native Ni and metal alloy Ni-Fe were found in syngenetic inclusions, which makes it possible to capture Ni ions in structural sites at elevated temperatures [61,62,64].

The radiation centers detected via the PL and EPR spectra are probably formed due to their own radiation sources contained in the original rock. In particular, monazite and other radiation sources have been diagnosed in shungite; monazite is also present in carbonado [18]. At the same time, the relatively low temperature of the destruction of these centers indicates the period of stay of the rock at even lower temperatures and additionally shows the possibility of the exhumation of diamond rocks.

Our hypothesis of the genesis of carbonado via subduction, exhumation, and exogenous reworking of former shungite fits the properties of carbonado most adequately and completely.

5. Conclusions

The diamond variety called "carbonado" has a micropolycrystalline structure, but not any diamond with such a structure can be classified as a carbonado. Unfortunately, the use of this feature alone has led to the "discovery" of carbonados in a wide variety of places on the planet and in a wide variety of geological settings. Due to this fact, it has not been possible to determine the genesis of carbonados so far.

To understand the genesis of carbonado, it is necessary to take into account the following: 1—the clastic form of its outcrops, indicating that they are fragments of a large geological body; 2—the high degree of mechanical wear, which, along with the isotopic age, indicates the antiquity of these diamonds: Archean or early Proterozoic; 3—genuine carbonados are an endemic variety of diamond, and they are distributed only in territories in Brazil and Central Africa, which, within Gondwana, were united and separated only in the Mesozoic due to the opening of the Atlantic.

This study suggests that the most likely precursor to carbonado is shungite or both carbonado and shungite originated from a similar precursor substance. It corresponds to carbonado in carbon isotope composition, age, and presence of mineral impurities. Shungite, which is known to be found in Karelia (Russia), was formed by biomass monocellular algae fallout at the bottom of ocean basins in the early Proterozoic and, after metamorphism, represented a large geologic body. Upon subduction, the shungite rock recrystallized into diamond rock with phenocrysts of other mineral matter contained in the original substance. The exhumation associated with folding and thrusting could bring the diamond rock to the surface of the Earth, similarly to the massifs of Kumdy-Kol (Kazakhstan), Beni-Boucher (Morocco), and Ronda (Spain), and the exogenous destruction and reworking of this body supplied the fragments that we find and call "carbonado". There are reports about the presence of nanodiamonds in shungite, which may contribute to the formation of carbonado [65,66]. Shungites were probably much more widespread earlier than they are now, but only one of the shungite bodies, submerged in the mantle and then exhumed, served as the source of the carbonados and determined their endemic character.

Author Contributions: Conceptualization, V.A., V.K., A.Y., R.M., S.G., S.U., E.B., O.I. and A.P.; methodology, V.A., V.K., A.Y., R.M., S.G., S.U., E.B., O.I. and A.P.; investigation, V.A., V.K., A.Y., R.M., S.G., S.U., E.B., O.I. and A.P.; writing—original draft preparation, V.A., R.M., A.Y. and S.U.; writing—review and editing, V.A. and S.U. All authors have read and agreed to the published version of the manuscript.

Funding: This work was supported by the state assignments of IGM SB RAS (No 122041400157-9), DPMGI SB RAS (FUFG-2024-0007), NIIC SB RAS (No 121031700313-8) and IG KarRC RAS (No 1022040400163-5).

Data Availability Statement: All the information on this study is presented in the article.

Acknowledgments: The authors are grateful to the Analytical Center for multi-elemental and isotope research SB RAS.

Conflicts of Interest: The authors declare no conflict of interest.

References

1. Leonardos, O.H. *Diamante e Carbonado do Estado da Bahia*; Departamento Nacional da Producção Mineral: Rio de Janeiro, Brazil, 1937; pp. 1–16.
2. Kaminsky, F.V.; Klyuev, Y.A.; Prokopchuk, B.I.; Shcheka, S.A.; Smirnov, V.I.; Ivanovskaya, I.N. The first finds of carbonado and a new find of ballas in the Soviet Union. *Dokl. Earth Sci. SSSR* **1978**, *242*, 687–689.
3. Argunov, K.P.; Zinchuk, N.N.; Zuev, V.M.; Kvasnitsa, V.N.; Melnrikov, V.S.; Sleptsov, V.V. Carbonado and defective crystals among small diamonds from kimberlites. *Mineral. J.* **1985**, *7*, 95–98.
4. Smith, J.V.; Dawson, J.B. Carbonado: Diamond aggregates from early impacts of crustal rocks? *Geology* **1985**, *13*, 342–343. [CrossRef]
5. Kaminsky, F.V.; Bartoshinsky, Z.V.; Koptil, V.I. Some questions of terminology of polycrystalline diamond aggregates. *Mineral. Collect.* **1987**, *41*, 16–20.
6. Gorshkov, A.I.; Seliverstov, V.A.; Baykov, A.I.; Anikin, L.P.; Sivtsov, A.V.; Dunin-Barkovsky, R.L. Crystal chemistry and genesis of carbonado diamonds from melanocratic basaltic of Avacha volcano in Kamchatka. *Geol. Rudn. Mestorozhd.* **1995**, *37*, 54–66.
7. Gorshkov, A.I.; Titkov, S.V.; Sivtsov, A.V.; Bershov, L.V.; Marfunin, A.S. First finds of native metals Cr, Ni, and αFe in carbonado from diamond deposits of Yakutia. *Geochemistry* **1995**, *4*, 588–591.
8. Titkov, S.V.; Gorshkov, A.I.; Vinokurov, S.F.; Bershov, L.V.; Solodov, D.I.; Sivtsov, A.V. Geochemistry and genesis of carbonado from Yakut diamond deposits. *Geochemistry* **2001**, *3*, 261–270.
9. Chumak, M.A.; Bartoshinsky, Z.V. Yakutite—A new variety of diamond. *Geol. Yakutia* **1968**, *27*, 29–38.
10. Orlov, Y.L. *The Mineralogy of the Diamond*; John Wiley & Sons: New York, NY, USA, 1977; p. 235.
11. Kaminsky, F.V. Carbonado and yakutite: Properties and possible genesis. In *International Kimberlite Conference: Extended Abstracts*; CPRM Special Publication: Rio de Janeiro, Brazil, 1991; pp. 136–143. [CrossRef]
12. Kagi, H.; Takahashi, K.; Hidaka, H.; Masuda, A. Chemical properties of Central African carbonado and its genetic implications. *Geochim. Cosmochim. Acta* **1994**, *58*, 2629–2638. [CrossRef]
13. Shibata, K.; Kamioka, H.; Kaminsky, F.V.; Koptil, V.I.; Svisero, D.P. Rare earth element patterns of carbonado and yakutite: Evidence for their crustal origin. *Mineral. Mag.* **1993**, *57*, 607–611. [CrossRef]
14. Gorshkov, A.I.; Bershov, L.V.; Vinokurov, S.F.; Oton, K.L.; Sivtsov, A.V.; Mokhov, A.V.; Bogacheva, E.O. Carbonado from Lencois district, Bahia state (Brazil): Mineral inclusions, physical properties, geochemical features and conditions of formation. *Geol. Ore Depos.* **1997**, *39*, 269–277.
15. Francesson, E.V.; Kaminsky, F.V. Carbonado—A variety of diamond of non-kimberlite genesis. *Rep. Acad. Sci. USSR* **1974**, *219*, 187–189.
16. Demény, A.; Nagy, G.; Garai, J.; Bajnóczi, B.; Németh TDrozd, V.; Hegner, E. Hydrogen isotope compositions in carbonado diamond: Constraints on terrestrial formation. *Cent. Eur. Geol.* **2011**, *54*, 51–74. [CrossRef]
17. Pokhilenko, N.P.; Shumilova, T.G.; Afanasyev, V.P.; Litasov, K.D. Diamonds in the Kamchatka peninsula (Tolbachik and Avacha volcanoes): Natural origin or contamination? *Geol. Geophys.* **2019**, *60*, 606–618. [CrossRef]
18. Trueb, L.F.; Butterman, W.C. Carbonado: A microstructural study. *Am. Mineral.* **1969**, *54*, 412–425.
19. Haggerty, S.E. Carbonado Diamond: A Review of Properties and Origin. *Gems Gemol.* **2017**, *53*, 168–179. [CrossRef]
20. Burgess, R.; Johnson, L.H.; Mattey, D.P.; Harris, J.W.; Turner, G. He, Ar and C isotopes in coated and polycrystalline diamonds. *Chem. Geol.* **1998**, *146*, 205–217. [CrossRef]
21. Chen, J.H.; Van Tendeloo, G. Microstructure of tough polycrystalline natural diamond. *J. Electron. Microsc.* **1999**, *48*, 121–129. [CrossRef]
22. Heaney, P.J.; Vicenzi, E.P.; De, S. Strange diamonds: The mysterious origins of carbonado and framesite. *Elements* **2005**, *1*, 85–89. [CrossRef]
23. Kagi, H.; Fukura, S. Infrared and Raman spectroscopic observations of Central African carbonado and implications for its origin. *Eur. J. Mineral.* **2008**, *20*, 387–393. [CrossRef]
24. Ishibashi, H.; Kagi, H.; Sakuai, H.; Ohfuji, H.; Sumino, H. Hydrous fluid as the growth media of natural polycrystalline diamond, carbonado: Implication from IR spectra and microtextural observations. *Am. Mineral.* **2012**, *97*, 1366–1372. [CrossRef]
25. Ketcham, R.A.; Koeberl, C. New textural evidence on the origin of carbonado diamond: An example of 3-D petrography using X-ray computed tomography. *Geosphere* **2013**, *9*, 1336–1347. [CrossRef]
26. De Carli, P.S. Carbonado origin: Impact vs. subduction. In Proceedings of the American Geophysical Union Meeting, Baltimore, MD, USA, 27–30 May 1997; p. S333.
27. Irifune, T.; Kurio, A.; Sakamoto, S.; Inoue, T.; Sumiya, H.; Funakoshi, K. Formation of pure polycrystalline diamond by direct conversion of graphite at high pressure and high temperature. *Phys. Earth Planet. Inter.* **2004**, *143–144*, 593–600. [CrossRef]

28. Ozima, M.; Zashu, S.; Tomura, K.; Matsuhisa, Y. Constraints from noble-gas contents on the origin of carbonado diamonds. *Nature* **1991**, *351*, 472–474. [CrossRef]
29. Daulton, T.L.; Ozima, M. Radiation-induced diamond formation in uranium-rich carbonaceous materials. *Science* **1996**, *271*, 1260–1263. [CrossRef]
30. Ozima, M.; Tatsumoto, M. Radiation-induced diamond crystallization: Origin of carbonados and its implications on meteorite nano-diamonds. *Geochim. Cosmochim. Acta* **1997**, *61*, 369–376. [CrossRef]
31. Haggerty, S.E. Diamond-carbonado: Models for a new meteorite class of circum-stellar or solar system origin. In Proceedings of the American Geophysical Union, Spring Meeting, Baltimore, MD, USA, 20–24 May 1996; p. S143.
32. Trueb, L.F.; De Wys, E.C. Carbonado: Natural polycrystalline diamond. *Science* **1969**, *165*, 799–802. [CrossRef]
33. Gorshkov, A.I.; Vinokurov, S.F.; Ryabchikov, I.D.; Bershov, L.V.; Magazina, L.O.; Sivtsov, A.V.; Solodov, D.I. Mineralogical and geochemical features of gold-bearing carbonado from Pochareu district, Mato Grosso state (Brazil). *Geochemistry* **2000**, *1*, 3–15.
34. Kaminsky, F.V.; Wirth, R.; Moralez, L. Internal texture and syngenetic inclusions in carbonado. *Can. Miner.* **2013**, *51*, 39–56. [CrossRef]
35. Jones, A.P.; Beard, A.; Milledge, H.J.; Cressey, G.; Kirk, C.; De Carli, P. A new nitride mineral in carbonado. In Proceedings of the Eighth International Kimberlite Conference, Victoria, BC, Canada, 22–27 June 2003; p. A95.
36. Vinogradov, A.P.; Kropotova, O.A.; Orlov, Y.L.; Grinenko, V.A. Isotopic composition of diamond and carbonado crystals. *Geochemistry* **1966**, *12*, 1385–1387.
37. Kaminsky, F.V.; Kirikilitsa, S.I.; Eremenko, G.K.; Polkanov, Y.A.; Khrenov, A.Y. New data on Brazilian carbonados. *Dokl. Earth Sci. USSR* **1979**, *249*, 443–445.
38. Sano, Y.; Yokochi, R.; Terada, K.; Chaves, M.L.; Ozima, M. Ion microprobe Pb–Pb dating of carbonado, polycrystalline diamond. *Precambrian Res.* **2002**, *113*, 155–168. [CrossRef]
39. Vins, V.G. New ultra-deep diamond cleaning technology. *GemsGemology* **2011**, *47*, 136.
40. Zaitsev, A.M. *Optical Properties of Diamond: A Data Handbook*; Springer: New York, NY, USA, 2001; p. 502.
41. Gippius, A.A.; Zaitsev, A.M.; Vavilov, V.S. Formation, annealing, and interaction of defects in ion-implanted layers of natural diamond. *Sov. Phys. Semicond. USSR* **1982**, *16*, 256–261.
42. Davies, G. *In Chemistry and Physics of Carbon*; Marcel Dekker: New York, NY, USA, 1977.
43. Loubser, J.H.N.; van Wyk, J.A. ESR in the study of diamond. *Rep. Progr. Phys.* **1978**, *41*, 1201–1248. [CrossRef]
44. Van Wyk, J.A. EPR of radiation damage centres W11, W12, W13 and W14 in type Ib diamond. *J. Phys. Condens. Matter* **1994**, *6*, 801–810.
45. Twitchen, D.J.; Newton, M.E.; Baker, J.M.; Tucke, O.D.; Anthony, T.R.; Banholzer, W.F. Electron-paramagnetic-resonance measurements on the di-<001>-split interstitial center in diamond. *Phys. Rev. B* **1996**, *54*, 6988–6998. [CrossRef]
46. Ammerlaan, C.A.J. *Paramagnetic Centers in Diamond. Landolt-Börnstein Numerical Data and Functional Relationships in Science and Technology, New Series III/22b*; Madelung, O., Schulz, M., Eds.; Springer: Berlin/Heidelberg, Germany, 2002; pp. 6–76.
47. Shames, A.I.; Osipov, V.Y.; von Bardeleben, H.J.; Vul', A.Y. Spin S = 1 centers: A universal type of paramagnetic defects in nanodiamonds of dynamic synthesis. *J. Phys. Condens. Matter* **2012**, *24*, 225302. [CrossRef]
48. Haggerty, S.E. Carbonado: Physical and chemical properties, a critical evaluation of proposed origins, and a revised genetic model. *Earth-Sci. Rev.* **2014**, *130*, 49–72. [CrossRef]
49. Afanasiev, V.P.; Pokhilenko, N.P.; Egorova, E.O.; Lindenblot, E.S. The oldest diamond crystals of the Siberian platform. *Dokl. Earth Sci.* **2019**, *489*, 77–81. [CrossRef]
50. Kovalevski, V.V.; Prikhodko, A.V.; Buseck, P.R. Diamagnetism of natural fullerene-like carbon. *Carbon* **2005**, *43*, 401–405. [CrossRef]
51. Tashiro, T.; Ishida, A.; Hori, M.; Igisu, M.; Koike, M.; Méjean, P.; Takahata, N.; Sano, Y.; Komiya, T. Early trace of life from 3.95 Ga sedimentary rocks in Labrador, Canada. *Nature* **2017**, *549*, 516–518. [CrossRef] [PubMed]
52. Morrison, J. New origin seen for Earth's tectonic plates. *Nature* **2014**. [CrossRef]
53. Bercovici, D.; Yanick, R. Plate tectonics, damage and inheritance. *Nature* **2014**, *508*, 513–516. [CrossRef]
54. Jones, N. Minerals yield signs of early plate tectonics for this period. *Nature* **2008**. [CrossRef]
55. Sobolev, N.V.; Shatsky, V.S.; Zayachkovsky, A.A.; Vavilov, M.A.; Sheshkel, G.G. *Diamonds in Metamorphic Rocks of Northern Kazakhstan: Geology of Metamorphic Complexes*; Ural Branch of the Russian Academy of Sciences: Sverdlovsk, Russia, 1989; pp. 21–35.
56. Shatsky, V.S.; Sobolev, N.V.; Zayachkovsky, A.A.; Zorin, Y.M.; Vavilov, M.A. New manifestation of microdiamonds in metamorphic rocks as evidence of the regional nature of ultra-high pressure metamorphism in the Kokchetav massif. *Dokl. Earth Sci. USSR* **1991**, *321*, 189–194.
57. Slodkevich, V.V. Paramorphoses of graphite on diamond. *Zap. VMO* **1982**, *1*, 13–33.
58. Pearson, D.G.; Davies, G.R.; Nixon, P.H.; Milledge, H.J. Graphitized diamonds from a peridotite massif in Morocco and implications for anomalous diamond occurrences. *Nature* **1989**, *338*, 60–62. [CrossRef]
59. Davies, G.R.; Nixon, P.N.; Pearson, G.D. Tectonic implications of graphitized diamonds from the Ronda peridotite massif, southern Spain. *Geology* **1993**, *21*, 471–474. [CrossRef]
60. Afanasiev, V.P.; Litasov, K.D.; Goryainov, S.V.; Kovalevsky, V.V. Raman spectroscopic analysis of nanopolycrystalline diamond, obtained from shungite at 15 GPa and 1600 °C. *Lett. J. Exp. Theor. Phys.* **2020**, *111*, 218–224. [CrossRef]

61. Yavkin, B.V.; Mamin, G.V.; Gafurov, M.R.; Orlinskii, S.B. Size-dependent concentration of N0 paramagnetic centres in HPHT nanodiamonds. *Magn. Reson. Solids.* **2015**, *17*, 15101.
62. Noble, C.J.; Pawlik, T.; Spaeth, J.-M. Electron paramagnetic resonance investigations of nickel defects in natural diamonds. *J. Phys. Condens. Matter* **1998**, *10*, 11781–11793. [CrossRef]
63. Shames, A.I.; Panich, A.M. Paramagnetic defects in nanodiamonds. In *Nanodiamonds*; Elsevier: Amsterdam, The Netherlands, 2017; pp. 131–154.
64. Isoya, J.; Kanda, H.; Norris, J.R.; Tang, J.; Bowman, M.K. Fourier-transform and continuous-wave EPR studies of nickel in synthetic diamond: Site and spin multiplicity. *Phys. Rev. B* **1990**, *4*, 3905–3913. [CrossRef] [PubMed]
65. Kovalevsky, V.V. Structural state of shungite carbon. *Zhurnal Neorg. Chem.* **1994**, *39*, 31–35.
66. Simakov, S.K. Physicochemical aspects of macro-, micro- and nano-sized diamond formation in nature. *Interdiscip. Sci. Appl. J. Biosph.* **2014**, *6*, 257–264.